



*Supplement of*

## **Constraining topsoil pesticide degradation in a conceptual distributed scatchment model with compound-specific isotope analysis (CSIA)**

**Sylvain Payraudeau et al.**

*Correspondence to:* Sylvain Payraudeau ([sylvain.payraudeau@engees.unistra.fr](mailto:sylvain.payraudeau@engees.unistra.fr))

The copyright of individual parts of the supplement might differ from the article licence.

**Contents**

	<b>S1 Hydro-climatic conditions</b>	<b>3</b>
	<b>S2 Catchment description, sampling and transect area extents</b>	<b>3</b>
	<b>S3 Farmer surveys</b>	<b>4</b>
5	<b>S4 Mass balance estimations</b>	<b>5</b>
	<b>S5 <math>\delta^{13}C</math> analysis</b>	<b>5</b>
	<b>S6 Hydrological model</b>	<b>6</b>
	S6.1 Conceptual model . . . . .	6
	S6.2 Infiltration and runoff . . . . .	6
10	S6.3 Percolation . . . . .	9
	S6.4 Lateral subsurface flow . . . . .	9
	S6.5 Evapotranspiration . . . . .	9
	S6.6 Transpiration . . . . .	10
	S6.7 Evaporation . . . . .	11
15	S6.8 Root growth . . . . .	12
	<b>S7 Agronomic model</b>	<b>12</b>
	S7.1 Crop cover and height . . . . .	12
	S7.2 Topsoil bulk density . . . . .	13
	S7.2.1 Bulk density on days with tillage . . . . .	13
20	S7.2.2 Bulk density on days without tillage . . . . .	13
	S7.3 Characteristic water contents and topsoil saturated hydraulic conductivity . . . . .	15
	<b>S8 Mass transfer model</b>	<b>15</b>
	S8.1 Mass phase distribution . . . . .	15
	S8.2 Volatilisation . . . . .	15
25	S8.3 Runoff mass . . . . .	17

	S8.4 Leachate mass . . . . .	17
	S8.5 Lateral mass flux . . . . .	17
	<b>S9 Degradation model</b>	<b>18</b>
	<b>S10Morris</b>	<b>19</b>
30	<b>S11Measured S-metolachlor concentrations and <math>\delta^{13}C</math> for weekly transects</b>	<b>22</b>
	<b>S12<math>K_{OC}</math> sensitivity</b>	<b>23</b>

S1 Hydro-climatic conditions

Summary temperature and reference evapotranspiration, obtained from MeteoFrance (Station no. 67516001), and summary rainfall and discharge (measured) are shown in Table S1.

Table S1. Summary hydrological and climatic conditions (Alvarez-Zaldivar et al., 2018).

2016	$P(mm/d)^a$	$P_{tot}(mm)^b$	$ETP(mm/d)^c$	$T(C)^d$	$Q(mm/d)^e$	% Wet Days <sup>f</sup>
April	2.7±4.6	82.2	2.2±0.8	9.1±2.9	0.6±0.6	67%
May	4.6±7.1	136.8	3.1±1.2	14±3.2	0.9±1.3	63%
June	4.8±7.0	145.6	3.7±1.2	17.6±2.9	1.2±1.2	80%

<sup>a</sup> Mean daily rainfall; <sup>b</sup> total rainfall; <sup>c</sup> mean daily reference evapotranspiration; <sup>d</sup> mean daily temperature; <sup>e</sup> mean daily discharge normalised by total catchment area; <sup>f</sup> percent of days in a month were rainfall occurred.

S2 Catchment description, sampling and transect area extents

Field data was collected from a 47 ha headwater catchment located in Alteckendorf, France (48° 47' 11.03"N, 7° 35' 0.46"E) (Alvarez-Zaldivar et al., 2018; Lefrancq et al., 2018). The mean catchment slope is  $6.7 \pm 4.7\%$  with an altitude ranging between 190 and 230 m.

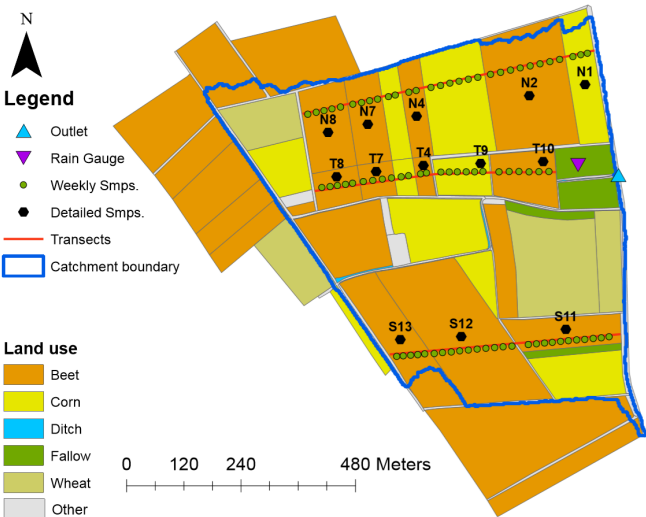
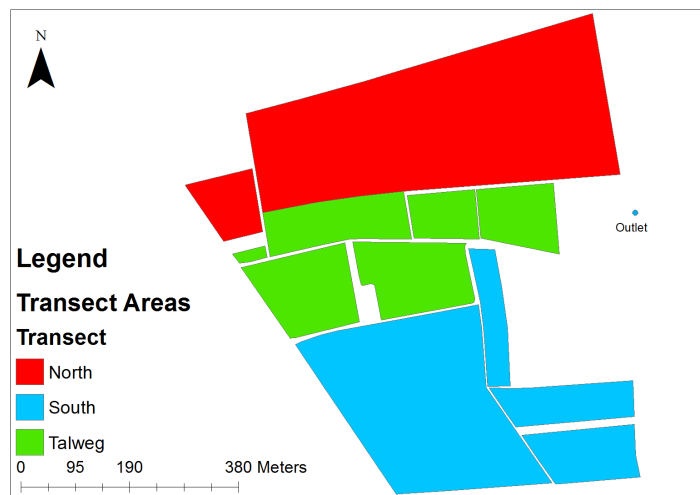


Figure S1. Transects (weekly) and plot (1, 50 and 100 days) catchment sampling. "Other" contains roads, grass strips and orchards



**Figure S2.** Delimited transect areas used to extrapolate remaining mass from soil concentrations measured for each transect sample weekly.

#### 40 S3 Farmer surveys

Three main applications (A1, A2, A3) were confirmed from farmer surveys and observations from weekly transect concentrations [S-metolachlor] and  $\delta^{13}\text{C}$  (Fig. S8). However, these concentration increases do not correspond with a significant decrease in  $\delta^{13}\text{C}$  that would be expected from a fresh application with a characteristic signature ( $\delta^{13}\text{C}_0 = -32.2 \pm 0.5\text{‰}$ ).

**Table S2.** Applied mass (Kg) of active ingredient (S-metolachlor) per transect by date and days since 1<sup>st</sup> application. Ranges indicates uncertainty of exact application date (Alvarez-Zaldivar et al., 2018).

App. No.	Date	Days	North	Valley	South
A1	March 20 - 25 <sup>th</sup>	0 - 5	5.1	1.6	11.1
A2	April 13 - 14 <sup>th</sup>	25 - 26	8.0	1.8	2.9
A3	May 25 - 31 <sup>st</sup>	67 - 73	7.2	2.4	0.0
Total (Kg)			20.2	5.9	14.0

#### S4 Mass balance estimations

45 *Soils.* Pesticide mass along a catchment's transect area  $M_{Tr,t}$  [ $\mu g$ ] is given by:

$$M_{Tr,t} = C_{Tr,t} \cdot \rho_{b_0} \cdot A_{Tr} \cdot D \quad (S1)$$

were  $C_{Tr}$  is the dry weight S-met soil concentration [ $\mu g/g$  soil dry wt] on transect  $Tr$  at time  $t$  and  $A_{Tr}$  is the associated transect area [ $m^2$ ] (Fig. S2) and  $D$  is sampling depth (1 cm). A homogeneous bulk density ( $\rho_{b_0} = 0.99 \text{ g/cm}^3$ ) was assumed based on sample measurements obtained across the catchment.

50 Transect signature and pesticide mass was then used to compute bulk signatures across the catchment ( $\delta^{13}C_{bulk}$ ) and given by:

$$\delta^{13}C_{bulk,t} = \sum_{Tr=1}^{TR=3} \frac{M_{Tr,t}}{M_{tot,t}} \delta^{13}C_{Tr,t} \quad (S2)$$

were  $\delta^{13}C_{Tr}$  is the S-met isotope signature in transect  $Tr$  and  $M_{tot}$  [ $\mu g$ ] the total catchment mass at time  $t$ .

*Outlet.* Outlet loadings (OL) [ $\mu g$ ] were calculated based on flow proportional samples given by:

$$55 \quad OL_{ws} = C_{ws} \int_t^{\Delta t} V(t) dt \quad (S3)$$

where  $C$  the concentration [ $\mu g/L$ ] of water sample  $ws$  and  $V$  [ $L$ ] is discharge over the sample time interval  $\Delta t$  [ $h$ ].

#### S5 $\delta^{13}C$ analysis

The GC-C-IRMS system consisted of a TRACE<sup>TM</sup> Ultra Gas Chromatograph (ThermoFisher Scientific) coupled via a GC IsoLink/Conflow IV interface to an isotope ratio mass spectrometer (DeltaV Plus, ThermoFisher Scientific). The carbon isotope ratios are reported in  $\delta$  notation [‰], using a three-point calibration against the Vienna Pee Dee Belemnite (V-PDB) standard (11237.2 · 10<sup>-6</sup>) and given by:

$$\delta^{13}C_{sample}[‰] = \frac{R_{sample} - R_{standard}}{R_{standard}} \cdot 1000 \quad (S4)$$

where  $R_{sample}$  and  $R_{standard}$  are the ratios  $^{13}C/^{12}C$  of sample and standard, respectively. Based on GC-IRMS linearity tests, the minimum peak amplitudes needed for accurate  $\delta^{13}C$  measurements was established as about 300 mV (Alvarez-Zaldivar et al., 2018), which correspond to 10 ng of carbon injected on column.

During chemical transformation, lighter isotopes (e.g.,  $^{12}C$ ) exhibit lower activation energy, generally resulting in faster reaction times relative to their heavier counterparts (e.g.,  $^{13}C$ ). This leads to an enrichment of the heavier isotopologues in the non-degraded pesticide fraction remaining in environmental samples (Elsner, 2010). The resulting average isotope value (e.g.,

$\delta^{13}C$ ) of the non-degraded fraction can then be used to quantify degradation by following the Rayleigh distillation equation (Rayleigh, 1986). Research on legacy contaminants (Hunkeler et al., 2008; Sherwood Lollar et al., 2011) and nitrate pollution (Nestler et al., 2011; Fenech et al., 2012), have shown CSIA to be a valuable complementary line of evidence to demonstrate degradation, persistence and source identification at various temporal and spatial scales. Akin to these approaches, application of CSIA to pesticides relies on the ability to monitor changes in stable isotope composition between source(s) and outlet to quantify the extent of (bio)chemical conversion at the catchment scale.

## S6 Hydrological model

### S6.1 Conceptual model

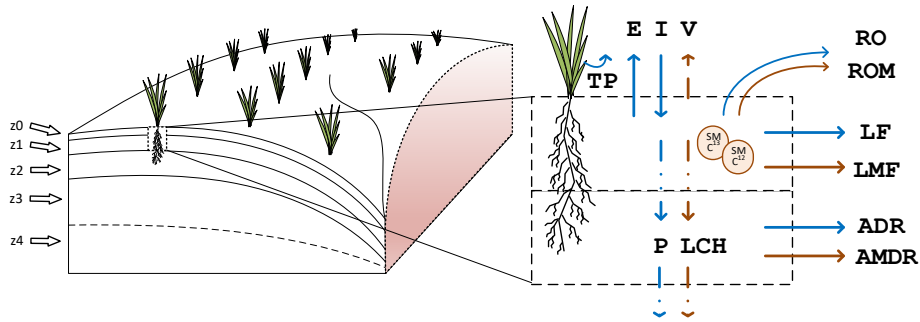


**Figure S3.** Conceptual 5-layer spatially distributed hydrological and reactive-transport PiBEACH model. Hydrological processes included evaporation (E), transpiration (TP), percolation (P) volatilization (V), runoff (RO), lateral flow (LF) and artificial drainage (ADR). Mass transfer processes included volatilization (V), runoff mass (ROM), lateral mass flow (LMF), leaching (LCH) and mass transfer through artificial drainage (AMDR)

### S6.2 Infiltration and runoff

To calculate infiltration,  $I$  (mm) and surface runoff,  $RO$  (mm), soil moisture conditions are determined by following the SCS curve number defined by the U.S. Soil Conservation Service (SCS, 1972). Infiltration is given by,

$$I = R - RO \quad (S5)$$

where  $R$  (mm) is rainfall. The run-off equation is given by (Neitsch et al., 2009):

$$RO = \begin{cases} 0, & R \leq I_a \\ \frac{(R - I_a)^2}{R - I_a + S}, & R > I_a \end{cases} \quad (S6)$$

**Table S3.** Full set of model parameters

Parameter	Units	Bounds	95% CI	Description	Source
Layers	-	5	-	Number of model layers	Conceptual
z0	mm	10	-	Layer depth	"
z1	mm	300	-	<i>ibid.</i>	"
z2	mm	500	-	<i>ibid.</i>	"
z3	mm	zDat · (zf)	-	Depth to datum (zDat), upper water table	"
z4	mm	zDat · (1-zf)	-	Depth to datum (zDat), lower water table	"
z <sub>f</sub>	-	0.75, 0.99	0.87, 0.99	z3 and z4 distribution fraction	Calibration
c <sub>z0z1</sub>	d <sup>-1</sup>	0, 1	0, 1	Lateral flow coefficient (Manfreda et al., 2005), z0, z1	"
c <sub>z2z3z4</sub>	d <sup>-1</sup>	0, 1	0.2, 0.6	<i>ibid.</i>	"
c <sub>adr</sub>	d <sup>-1</sup>	0, 1	0.03, 0.92	Drainage lateral flow coefficient	"
K <sub>G</sub>	d	1100, 3650	1522, 3650	Linear reservoir constant regulating baseflow discharge	"
γ <sub>z0z1</sub>	-	0, 1	0.32, 1	log(K <sub>sat</sub> ) adjustment factor for layer (z)	"
γ <sub>z2z3</sub>	-	0, 1	0, 0.81	<i>ibid.</i>	"
K <sub>sat,z0z1</sub>	mm d <sup>-1</sup>	112.9, 781.8	-	Saturated hydraulic conductivity (adjusted by γ)	Agro. model
K <sub>sat,z1z2z3</sub>	-	643.2	-	<i>ibid.</i>	"
θ <sub>WP</sub>	-	0.19	-	Wilting point, all layers; 0.16 ± 0.03	"
θ <sub>FC,z0z1</sub>	-	0.37, 0.40	-	Field capacity, plow layer (0 - 300 mm); 0.37 ± 0.01	"
θ <sub>SAT,z0z1</sub>	-	0.49, 0.63	-	Saturation capacity, plow layer; 0.57 ± 0.04	"
θ <sub>FC,z2z3z4</sub>	-	0.37	-	Field capacity, z < 310 mm depth; 0.37 ± 0.03	Field charac.
θ <sub>SAT,z2z3z4</sub>	-	0.57	-	Saturation capacity, z < 310 mm depth; 0.57 ± 0.04	"
f <sub>transp</sub>	-	0, 1	0.38, 1	Adjustment factor, transpiration	Calibration
f <sub>evap</sub>	-	0, 1	0.1, 0.88	Adjustment factor, evaporation	"
p <sub>bAgr,z0z1</sub>	g cm <sup>-3</sup>	0.98, 1.36	-	Soil bulk density ; 1.17 ± 0.11	Agro. model
p <sub>b,z2,z3,z4</sub>	g cm <sup>-3</sup>	1.5	-	Soil bulk density, below plough layer; 1.5 ± 0.09	Field charac.
f <sub>oc</sub>	kg kg <sup>-1</sup>	0.01, 0.05	0.01, 0.05	Fraction of organic carbon (Lefrancq et al., 2018)	Calibration
K <sub>oc</sub>	mlg <sup>-1</sup>	0.3, 16180	0.3, 2000	Adsorption coefficient (Boitias et al., 2014; European Commission, 2004; Kollman et al., 1995; Lefrancq et al.; 2018 NCBI, 2017)	"
K <sub>d</sub>	mlg <sup>-1</sup>	0.003, 809	0.003, 76.9		"
β <sub>runoff</sub>	mm	0, 1	0, 0.4	Calibration constant for runoff mass transfer (Ahuja et al., 1983)	"
K <sub>age</sub>	d	0.0002, 0.07	0.0002, 0.005	Ageing rate, controls mass movement to non-bioavailable fraction	"
K <sub>irs</sub>	d	0.002, 0.01	0.002, 0.009	Rate of irreversible sorption / loss of recoverable fraction	"
DT <sub>50,ref</sub>	d	1, 50	9.2, 24.9	Ref. degradation half-life	"
ε <sub>iso</sub>	-	-4.0, -1.0	-3.467, -1.721	Enrichment factor	"
β <sub>θ</sub>	-	0, 1	0.03, 1.0	Constant exponent, degradation factor (Walker et al., 1974)	"

Parameters removed from hypercube sampling after Morris sensitivity included water content at -100 cm (W100 all layers); wilting point (all layers: θ<sub>WP</sub>); field capacities (θ<sub>FC,zX</sub>) and saturation capacities (all layers: θ<sub>SAT,zX</sub>)



where  $I_a$  (mm) is the initial abstraction capacity of the surface layer, which includes surface storage, interception and infiltration prior to runoff, and typically ranges from 0.05S to 0.2S. The model adopts the latter of these values as it has provided reliable results for previous rainfall-runoff events (Lim et al., 2006). S (mm) is the retention parameter after run-off given as a function of the soil profile water content:

$$S = S_{max} \cdot \left(1 - \frac{SW}{(SW + \exp[w_1 - w_2 \cdot SW])}\right) \quad (S7)$$

where  $w_1$  (mm) and  $w_2$  (-) are shape coefficients, SW (mm) is the soil profile water content of the first two layers,  $z_0$ ,  $z_1$ , excluding the amount of water held in the soil profile at wilting point such that:

$$SW = \max \left[ \left\{ \left( \frac{D_{z0}\theta_{z0} + D_{z1}\theta_{z1}}{D_{z0} + D_{z1}} - \theta_{wp} \right) \cdot (D_{z0} + D_{z1}) \right\}, \{0\} \right] \quad (S8)$$

and  $S_{max}$  (mm) is the maximum value that the retention parameter can take such that:

$$S_{max} = 254 \cdot \left( \frac{100}{CN_1} - 1 \right) \quad (S9)$$

Calculation of  $w_1$  and  $w_2$  is given by,

$$w_1 = \ln \left[ \frac{FC}{\left(1 - \frac{S_3}{S_{max}}\right)} - FC \right] + w_2 \cdot FC \quad (S10)$$

95

$$w_2 = \frac{\ln \left[ \frac{FC}{\left(1 - \frac{S_3}{S_{max}}\right)} - FC \right] - \ln \left[ \frac{SAT}{\left(1 - \frac{2.54}{S_{max}}\right)} - SAT \right]}{SAT - FC} \quad (S11)$$

where FC (mm) is the soil profile water content at field capacity,  $S_3$  (mm) is the retention parameter corresponding to field capacity (i.e. CN3) and SAT (mm) is the soil profile water content at saturation.  $S_3$  is given by:

$$S_3 = 254 \cdot \left( \frac{100}{CN_3} - 1 \right) \quad (S12)$$

100 CN numbers depend on permeability, land use, slope and antecedent moisture conditions. Curve numbers are classified according to three moisture conditions: dry (wilting point -  $CN_1$ ), average moisture ( $CN_2$ ) and wet (field capacity -  $CN_3$ ). Typical  $CN_2$  numbers for various land covers, hydrologic conditions and soil types at a 5% slope are given in Neitsch et al. (2009).  $CN_2$  values are used to derive  $CN_3$  before slope adjustment,

$$CN_3 = CN_2 \cdot \exp[0.00673 \cdot (100 - CN_2)] \quad (S13)$$

105 Before plugging eq. S13 into eq. S12, adjustment to local slope of  $CN_2$  is required,

$$CN_{2s} = \frac{CN_3 - CN_2}{3} \cdot [1 - 2 \cdot \exp(-13.86 \cdot slope)] + CN_2 \quad (S14)$$

where  $CN_{2s}$  is the curve number for average moisture conditions adjusted to the local slope.  $CN_1$  values accounting for slope are then calculated as:

$$CN_1 = CN_{2s} - \frac{20 \cdot (100 - CN_{2s})}{\left(100 - CN_{2s} + \exp[2.533 - 0.0636 \cdot (100 - CN_{2s})]\right)} \quad (S15)$$

- 110 Finally, recalculation of eq. S13, replacing  $CN_2$  with  $CN_{2s}$  to adjust for local slope, is done before plugging  $CN_3$  back into eq. S12.

### S6.3 Percolation

Percolation (P) is assumed to be negligible at moisture levels below field capacity. Above field capacity, percolation is given by Raes (2002):

$$115 \quad P_z = D_z \tau_z (\theta_{sat,z} - \theta_{fc,z}) \frac{e^{\theta_z - \theta_{fc,z}} - 1}{e^{\theta_{sat,z} - \theta_{fc,z}} - 1}, \text{ if } \theta_z > \theta_{fc,z} \quad (S16)$$

where  $D_z$  (mm) is the soil profile depth of layer  $z$  and  $\tau$  is a dimensionless drainage characteristic given by:

$$\tau = 0.0866 \cdot e^{\gamma_z \cdot \log_{10}(K_{sat})}, \quad 0 < \tau \leq 1 \quad (S17)$$

where  $\gamma_z$  (-) is a calibration coefficient and  $K_{sat}$  (mm d<sup>-1</sup>) is the saturated hydraulic conductivity.

### S6.4 Lateral subsurface flow

- 120 Lateral flow ( $LF_{z_i}$ ) (mm) occurs when the soil moisture content exceeds the field capacity ( $f_{pot_i}$ ) at each upstream cell ( $i$ ) and the receiving downstream cell has available pore space capacity ( $f_{cap_j} > 0$ ). The total flux at each cell is given by,

$$LF_{z_i} = \min(f_{pot_i}, f_{cap_j}) \cdot D_z \quad (S18)$$

$$f_{pot_i} = c_z \cdot (\theta_t - \theta_{fc}) \quad (S19)$$

125

$$f_{cap_j} = \frac{\theta_{sat_z} - \theta_{t_z}}{\sum_{i=1}^I (i)} \quad (S20)$$

where  $c_z$  (d<sup>-1</sup>) is a subsurface flow coefficient analogous to Manfreda et al., (2005),  $f_{cap_j}$  (-) the soil water capacity of the downstream cell,  $\sum_{i=1}^I (i)$  is the sum of upstream contributors and

### S6.5 Evapotranspiration

- 130 To account for evapotranspiration processes the FAO56 reference evaporation rate,  $ET_0$  (mm), has been considered and adjusted dynamically according to crop and climate-specific factors. The approach assumes a dual crop coefficient approach

appropriate for daily time-step calculations (Allen et al., 1998) and made up of a basal crop coefficient ( $K_{cb}$ ) and a soil water evaporation coefficient ( $K_e$ ). Potential evapotranspiration ( $ET_p$ ) is then given by

$$ET_p = K_c \cdot ET_0 \quad (S21)$$

135

$$K_c = K_{cb} + K_e \quad (S22)$$

where  $K_{cb}$  varies according to crop-specific development stage. In cases where the mean value for daily relative humidity during the mid- or late-season growth stage ( $RH_{min}$  %) differs from 45% or where wind speed varies by more than 2 m/s the  $K_{cb}$  values for mid- and late-season must be adjusted according to:

$$140 \quad K_{cb} = K_{cb_{mid/end}} + \left[ 0.04(U_2 - 2) - 0.004(RH_{min} - 45) \right] \left( \frac{h_{crop}}{3} \right)^{0.3} \quad (S23)$$

$$K_e = K_{cmax} - K_{cb} \quad (S24)$$

where  $K_{cb_{mid/end}}$  represent the reference values for sub-humid climate and moderate wind speeds (Allen et al., 1998).  $U_2$  is the wind speed at a height of 2 meters (m/s),  $RH_{min}$  is the minimum relative humidity (%) and  $h_{crop}$  is crop height. The soil evaporation coefficient,  $K_e$ , and  $K_{cmax}$  (-) represents an upper limit to evapotranspiration from cropped surfaces (1.05 to 1.30) and given by Allen et al. (1998):

$$K_{cmax} = \max \left[ \left\{ K_{cb} + 0.05 \right\}, \left\{ 1.2 + [0.04(U_2 - 2) - 0.004(RH_{min} - 45)] \cdot \left( \frac{h}{3} \right)^{0.3} \right\} \right] \quad (S25)$$

## S6.6 Transpiration

To account for potential transpiration processes, water uptake by roots is considered and regulated by atmospheric demand and soil water content. When there is sufficient water in the soil, potential transpiration ( $T_p$ ) equals atmospheric demand (Allen et al., 1998):

$$T_p = K_{cb} \cdot ET_0 \cdot f_{tr} \quad (S26)$$

$ET_0$  is corrected here by including a calibration coefficient  $f_{tr}$  (-). Potential transpiration is further subject to root water uptake capacity where the maximum daily uptake  $T_{p(z)}$  (mm) at each layer  $z$  is given by (Prasad, 1988):

$$155 \quad T_{p(z)} = 2 \left( 1 - \frac{RD_{z/2}}{RD} \right) \left( \frac{RD_z}{RD} \right) T_p \quad (S27)$$

where  $RD$  (mm) and  $RD_z$  (mm) are the total and the soil layer's rooting depth, respectively and  $RD_{z/2}$  is the soil depth at the middle of the root extension for layer  $z$ .

When soil water is insufficient to meet atmospheric demand, actual transpiration is lower than potential transpiration and given by Allen et al. (1998):

$$160 \quad T_{a(z)} = K_s \cdot T_p \quad (S28)$$

$$K_s = \max \left[ 0, \min \left( 1, \frac{\theta_t - \theta_{wp}}{\theta_c - \theta_{wp}} \right) \right] \cdot f_{transp} \quad (S29)$$

$$\theta_c = \theta_{wp} + (1 - p)(\theta_{fc} - \theta_{wp}) \quad (S30)$$

165

$$p = p_{tab} + 0.04(5 - ET_p) \quad (S31)$$

where  $K_s$  is a transpiration reduction parameter (0-1), which depends on soil water content,  $\theta_t$  ( $m^3/m^3$ ) and the critical soil moisture content  $\theta_c$  ( $m^3/m^3$ ) that defines the transition between unstressed and stressed transpiration rate. The the fraction of total depletable soil water is given by  $p$  (-) and the depletion factor (-)  $p_{tab}$ , for  $ET_p \approx 5 \text{ mm/d}$  (Allen et al., 1998)[Table no.

170 22].

## S6.7 Evaporation

Evaporation is considered only on bare surfaces and assumed to be negligible under plant cover and regulated by atmospheric deman along the first  $\approx 0.15 \text{ m}$  of soil (Sheikh et al., 2009). Considering the difference between actual ( $E_a$ , mm/d) and potential evaporation ( $E_p$ , mm/d) (Allen et al., 1998):

$$175 \quad E_p = K_e \cdot ET_0 \quad (S32)$$

$$E_a = K_r \cdot E_p \quad (S33)$$

where  $K_r$  is an evaporation reduction coefficient (-) given by:

$$K_r = \frac{\theta_t - \theta_{dr}}{\theta_{fc} - \theta_{dr}} \quad (S34)$$

180 where  $\theta_t$  is soil moisture ( $m^3/m^3$ ) and  $\theta_{dr}$  is the moisture ( $m^3/m^3$ ) of air-dry soil.

## S6.8 Root growth

Development of the root's depth followed that of Allen et al. (1998), which adjusts the crop's maximum root depth relative to the plant's development stage, where the total root depth  $D_{root}$  is given by,

$$RD = \begin{cases} 0, & J_t < J_{start} \\ RD_{min} + \left( RD_{max} - RD_{min} \right) \cdot \frac{J_t - J_{sow}}{J_{mid} - J_{start}}, & J_{sow} \leq J_t < J_{max} \\ D_{root,max}, & J_t > J_{max} \end{cases} \quad (S35)$$

185 where  $RD_{min}$  (mm) is the seed depth at sowing time in Julian days  $J_{sow}$  (d) and  $J_{mid}$  (d) the day at which the plant attains maximum rooting depth, typically at the mid-development stage. Crop development stage duration ( $L_{stage}$ ) (d) are also provided by Allen et al. (1998) for different crops. The Julian days corresponding to each stage are then given by,

$$J_{stage} = J_{sow} + L_{ini} = J_{dev} \quad J_{dev} + L_{dev} = J_{mid} \quad J_{mid} + L_{mid} = J_{late} \quad J_{late} + L_{end} = J_{end} \quad (S36)$$

## S7 Agronomic model

### 190 S7.1 Crop cover and height

Crop cover is calculated according to an asymptotic sigmoid function similar to the biomass production function of Hunt (1982), and which uses the degree-day (DD) approach defined as the difference between daily mean temperature and a crop-dependent base temperature for crop development,

$$COV(t) = \frac{COV_{max}}{1 + \frac{COV_{max} - COV_{ini}}{COV_{ini}} \cdot \exp(-COV_{max} \cdot f \cdot \frac{\sum DD}{\sum DD_{COV_{max}}})} \quad (S37)$$

$$195 \quad DD_{base} = T - T_{base}, (T \geq T_{base}) \quad 0, \quad (T < T_{base}) \quad (S38)$$

where,

$COV(t)$ : crop cover on day  $t$  (%);

$COV_{max}$ : crop dependent maximum crop cover (%);

$COV_{ini}$ : initial crop cover ( $0 < COV_{ini} < 1\%$ , here  $0.5\%$ );

200  $f$ : shape parameter ( $\approx 0.07$ );

$DD$ : degree-day ( $^{\circ}C$ );

$\sum DD$ : sum of  $DD$  on day  $t$  (since sowing);

$\sum DD_{COV_{max}}$ : crop dependent sum of  $DD$  since sowing necessary to reach the maximum crop cover ( $COV_{max}$ );

$T$ : daily mean temperature ( $^{\circ}C$ );

205  $T_{base}$ : crop dependent minimum daily mean temperature necessary for its development ( $^{\circ}C$ ).

We only consider temperature as a limiting factor for crop development; water and nutriment deficits are not accounted for. Crop height,  $H_v(t)$ , is calculated using the same equation with  $COV_{max}$  and  $C_{ini}$  replaced by analogous crop height parameters ( $H_{max}$  and  $H_{ini}$ ).

## S7.2 Topsoil bulk density

210 Topsoil bulk density has a strong dynamic character on arable land due to tillage, wheel traffic, root development, biological activity, rainfall impacts, shrinking and swelling, freezing and thawing. In this study we address the effects of tillage and rainfall on dry bulk density using methods inspired by those of the WEPP model (Alberts et al., 1995). First, a consolidated soil matrix density ( $BD_m$ ) is calculated using the pedotransfer functions (PTF) of Saxton and Rawls (2006) as a function of soil texture and soil organic matter content. Then tillage and rainfall effects are taken into account as detailed below.

### 215 S7.2.1 Bulk density on days with tillage

On days with tillage, the topsoil soil bulk density ( $BD_t$ ) is calculated as,

$$BD_t = BD_{t-1} - F_d BD_{t-1} + \frac{2}{1 + S_{tx}} F_d \frac{3}{4} BD_m \quad (S39)$$

where:

$BD_m$ : soil matrix density ( $\text{g cm}^{-3}$ ) obtained from the FTP of Saxton and Rawls (Saxton2006);

220  $BD_{t-1}$  and  $BD_t$ : bulk density at resp. day  $t - 1$  and day  $t$  ( $\text{g cm}^{-3}$ );

$F_d$ : surface fraction disturbed by tillage (-), determined from lookup tables of the WEPP model (Alberts et al., 1995);

$S_{tx}$ : soil texture related parameter accounting for particle cohesion effects (-), with  $S_{tx} < 1$  for sandy soils and  $> 1$  for clayey soils (USDA, 2003). Its value is determined from soil texture classes using lookup tables of the RUSLE model (USDA,2003).

225 Thus according to equation S39, tillage reduces the bulk density to 75% of the consolidated soil matrix density for silty soils and tillage affecting the entire surface. This factor is based on bulk density measurements directly after tillage compared to values obtained by the end of the growing season before crop harvest.

### S7.2.2 Bulk density on days without tillage

On rainy days without tillage, rainfall impact on topsoil bulk density is calculated as a function of the bulk density of the day  
230 before, the rainfall on day  $t$ , a soil stability factor ( $S_{stab}$ ), wheel track compaction (wt) and soil cover by either vegetation or crop residues according to,

$$BD_{bs,t} = BD_{bs,t-1} + (BD_m - BD_{bs,t-1})(1 - \exp(\frac{-R_t}{S_{stab}})) \quad (S40)$$

$$BD_{resi,t} = BD_{resi,t-1} + (BD_m - BD_{resi,t-1}) \left(1 - \frac{2 + \exp\left(\frac{R_t}{S_{stab}}\right)}{3}\right) \quad (S41)$$

$$BD_{crop,t} = \frac{BD_{resi,t} + BD_{bs,t}}{2} \quad (S42)$$

$$235 \quad BD_{wt,t} = 1.15 \cdot BD_m \quad (S43)$$

where,  $BD_{bs}$ ,  $BD_{resi}$ ,  $BD_{crop}$ ,  $BD_m$  ( $\text{g cm}^{-3}$ ) are respectively, topsoil bulk density of bare soil surface parts (bs), parts covered with crop residues (resi), parts covered with living crop (crop), and wheel tracks (wt);

$R_t$ : rainfall on day t (mm);

The soil stability factor  $S_{stab}$  (-) is derived from the crusting index of Rémy and Marin-Lafliche (1974) and is defined as:

$$240 \quad S_{stab} = 1000/I_C \quad (S44)$$

$$I_C = 5(I_S - 0.2) \quad (S45)$$

$$I_S = \frac{1.5FS + 0.75CS}{Clay + 10SOM} - Y \quad (S46)$$

$$Y = 0.2(pH - 7), (pH > 7) \quad 0, \quad (pH \leq 7) \quad (S47)$$

where:

245  $IS$ : soil stability index (-);

$IC$ : crusting index (-);

$FS$ : fine silt content (%);

$CS$ : coarse silt content (%);

$Clay$ : clay content (%);

250  $SOM$ : top soil organic matter content (%).

### S7.3 Characteristic water contents and topsoil saturated hydraulic conductivity

The regression PTFs of Saxton and Rawls (2006) were used to calculate the topsoil water contents at saturation ( $\theta_{sat}$  at 0 kPa moisture tension), wilting point ( $\theta_{wp}$  at 1500 kPa) and field capacity ( $\theta_{fc}$  at 33 kPa) by injecting the above modeled bulk densities per surface type (wheel track, bare soil, residue-covered and crop-covered surfaces). Then for each surface type, the  
255 saturated hydraulic conductivity is derived from Saxton and Rawls (2006),

$$K_{sat} = 1930(\theta_{sat} - \theta_{wp})^{3-\lambda} \quad (S48)$$

with  $\lambda$  being the slope of the logarithmic tension-moisture curve (-), determined using  $\theta_{fc}$  and  $\theta_{wp}$ . The final  $K_{sat}$  at the field scale is calculated as the weighted average of  $K_{sat}$ , the weight depending on the within-field surface fraction occupied by each of the four surface types.

## 260 S8 Mass transfer model

### S8.1 Mass phase distribution

Mass distribution at time  $t$  is given by,

$$M_{tot}(t) = V_{gas}c_{gas} + V_{H_2O}(t)c_{aq}(t) + M_{soil}(t)c_{ads}(t) \quad (S49)$$

where  $c_{aq}$  ( $\mu g L^{-1} H_2O$ ),  $c_{ads}$  ( $g Kg^{-1}$  soil),  $c_{gas}$  ( $\mu g L^{-1}$  air) are the dissolved, adsorbed and gaseous S-metolachlor  
265 concentrations, respectively and where  $c_{ads} = c_{aq}K_d$  and  $c_{gas} = c_{aq}/K_H^{cc}$ .  $V_{gas}$  and  $V_{H_2O}$  are the unsaturated and saturated pore space volume (L), respectively and  $M_{soil}$  is the soil mass (Kg).

### S8.2 Volatilisation

Pesticide volatilisation is only considered on the day of application and follows Leistra et al. (2001), where a boundary air layer is conceptualised through which pesticide diffuses before escaping into the atmosphere. The thickness ( $d_a$ ,  $m$ ) of this layer,  
270 was assumed to be equivalent to the topmost soil layer's thickness (10 mm) and regulates the transport resistance ( $r_a$ ,  $d/m$ ) such that:

$$r_a(t) = \frac{d_a}{D_a(t)} \quad (S50)$$

where  $D_a$  ( $m^2/d$ ) is the diffusion coefficient in air for Metolachlor at the observed environmental temperature and adjusted relative to the reference diffusion coefficient ( $D_{a,r}$ ,  $m^2/d$ ) as:

$$275 \quad D_a(t) = \left( \frac{T(t)}{T_r} \right)^{1.75} D_{a,r} \quad (S51)$$



where  $T$  and  $T_r$  are the environmental temperature at time  $t$  and at the reference temperature at 293.15°K, respectively.

The total volatilization is given by the flux across the air layer boundary ( $J_{v,air}$ ) and the flux across the topmost soil layer ( $J_{v,soil}$ ) such that:

$$J_{v,air}(t) = -\frac{C_{gas,top}(t) - C_{air}(t)}{r_a} \quad (S52)$$

$$280 \quad J_{v,soil}(t) = -\frac{C_{gas,z_0}(t) - C_{gas,top}(t)}{r_s} \quad (S53)$$

where  $C_{gas,top}$  ( $mg/m^3$ ) is the concentration in gas phase at the soil surface,  $C_{air}$  ( $mg/m^3$ ) the concentration in air,  $C_{gas,z_0}$  ( $mg/m^3$ ) the concentration in gas phase at the center of the uppermost soil layer and  $r_s$  ( $d/m$ ) the diffusion resistance across the topmost soil layer and given by:

$$r_s(t) = \frac{0.5D_z}{D_{rdiff,g}(t)} \quad (S54)$$

285 To calculate the relative diffusion ( $D_{rdiff,gas}$ ,  $m^2/d$ ) the model provides two options. Under option 1 (Millington and Quirk, 1960),

$$D_{rdiff,gas} = \frac{D_a(t) \left( \theta_{gas_z}(t) \right)^a}{\left( \theta_z(t) \right)^b} \quad (S55)$$

where Jin and Jury (1996) recommend that  $a = 2$  and  $b = 2/3$ . Under option 2 (Currie, 1960),

$$D_{rdiff,gas} = D_a(t) \left( a \right) \left( \theta_{gas_z}(t) \right)^b \quad (S56)$$

290 where Bakker et al. (1987) recommend  $a = 2.5$  and  $b = 3$  for moderately aggregated plough layers of loamy soils and humic sandy soils (Leistra et al., 2001).

Finally, it is assumed that flux across both layer boundaries is equivalent ( $J_{v,soil} = J_{v,air}$ ) (Leistra et al., 2001). Considering pesticide concentration in air to be negligible ( $C_{air} = 0$ ), the concentration at the soil surface is:

$$C_{gas,top}(t) = \frac{r_a}{(r_a + r_s)} C_{gas,z_0}(t) \quad (S57)$$

295 The gas concentration in the soil layer is related to the dimensionless Henry constant ( $K_H$ ), where:

$$C_{gas,z_0}(t) = C_{aq,z_0}(t) K_H \quad (S58)$$

Substituting eq. S57 into eq. S52 yields the mass flux lost to the atmosphere ( $g/m^2d$ ):

$$J_{v,air} = -\frac{C_{gas,z_0}}{(r_a + r_s)} \quad (S59)$$

### S8.3 Runoff mass

300 The non-uniform mixing-layer model is adapted from Ahuja and Lehman (1983) (see Shi et al., 2011), eq. 1 and p. 1217) and given by:

$$\frac{\partial(EDI \cdot \theta \cdot C_{aq})}{\partial t} = -ROe^{(-\beta_{RO} \cdot D_{z0})}C_{aq} \quad (S60)$$

where the Effective Depth of Interaction (EDI) refers to the mixing layer depth ( $mm$ ),  $\theta$  is soil moisture ( $m^3 m^{-3}$ ), RO is run-off ( $mm$ ) and  $C_{aq}$  is concentration in the mixing layer ( $g L^{-1}$ ). The parameter  $\beta_{RO}$  is a calibration constant (assuming,  
305  $1 \geq \beta > 0$ ) and where  $D_{z0}$  is the depth ( $mm$ ) of the top-soil layer.

### S8.4 Leachate mass

Vertical flux can be computed differently across soil layers. Under the first approach, and only for the uppermost layer, the model follows McGrath et al. (2008):

$$C_{z0,aq}(t+1) = C_{z0,aq}(t)exp\left(\frac{-P(t)}{\theta_{z0}(t) \cdot RET_{z0}(t) \cdot D_{z0}}\right) \quad (S61)$$

310 where the retardation factor,  $RET_z$  (-), is given by:

$$RET_z(t) = 1 + \frac{\rho_{bz}(t) \cdot K_d}{\theta_z(t)} \quad (S62)$$

The mass leached ( $g$ ) is thus given by:

$$M_{z0,lch}(t) = D_{z0} \cdot A_i \left( \theta_{z0}(t)C_{z0,aq}(t) - \theta_{z0}(t+1)C_{z0,aq}(t+1) \right) \quad (S63)$$

where  $A$  is the area ( $m^2$ ) for each cell  $i$ . For subsurface layers (i.e.,  $z > 0$ ), mass leached is proportional to the aqueous  
315 concentration in percolated water such that,

$$M_{z,lch}(t) = P_z(t) \cdot C_{z,aq}(t) \cdot A_i \quad (S64)$$

### S8.5 Lateral mass flux

Similarly to vertical mass flux, later mass flux is proportional to lateral water flow and the aqueous concentration at each cell  $i$ ,

$$M_{z,lf}(t) = LF_{zi}(t) \cdot C_{zi,aq}(t) \cdot A_i \quad (S65)$$

To account for changes in DT50 (days) due to changes in soil moisture, models from Walker (1974) and Schroll et al. (2006) where compared and evaluated against DT50 values derived from microcosm degradation experiments conducted at different temperatures ( $^{\circ}\text{C}$ ) and moistures ( $\text{m}^3 \text{ m}^{-3}$ ). Observed DT50 values were:  $DT50_{ref} = 30$  at  $\theta = 0.2$ ,  $T = 20$  (used as reference for validation);  $DT50 = 41$  at  $\theta = 0.4$ ,  $T = 20$ ;  $DT50 = 30$  at  $\theta = 0.4$ ,  $T = 30$ ). Although both methods mostly  
325 underestimated measured DT50 (Fig. S4), Walker’s approach resulted in smaller error differences and was selected for model implementation.

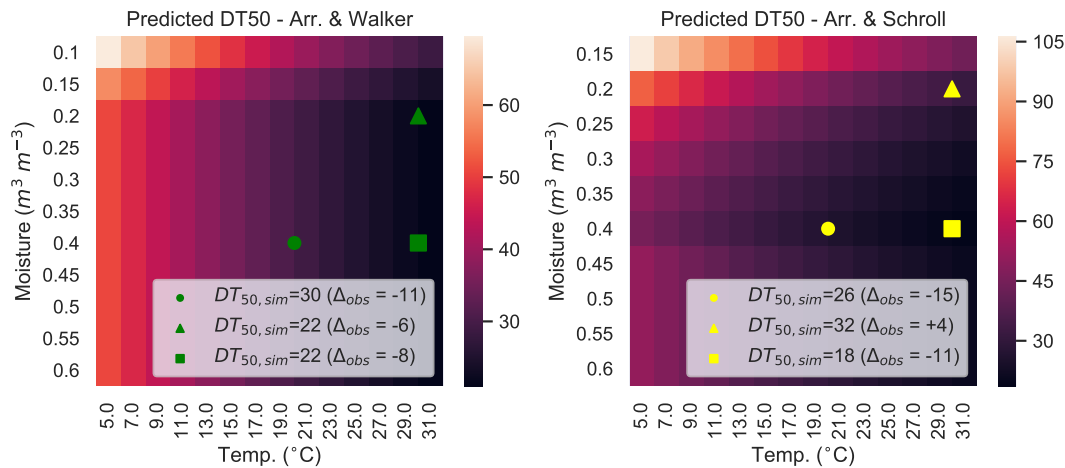


**Figure S4.** Calculated DT50 from Walker (1974) and Schroll et al. (2006) and differences to observed ( $\Delta_{obs}$ ) DT50 values from S-metolachlor microcosm degradation experiments. Both approaches follow Boesten and van der Linden (1991) for adaptation to the Arrhenius equation.

## S10 Morris

Morris is a global sensitivity analysis method based on calculation of elementary effects or EEs (see Morris, 1991 and Campolongo et al., 2007). Two sensitivity measures are the mean and SD of the EEs. The mean estimates the overall effect of each parameter on the output and the SD estimates interaction between inputs. Namely, if the mean of a given parameter  $i$  is different (relatively) from zero, it indicates that parameter  $i$  has an important "overall" influence on the output. A large SD implies that parameter  $i$  has a nonlinear effect on the output, or that there are interactions between parameter  $i$  and other parameters.

Figures S5 and S6 shows sensitivity results for S-metolachlor concentration and isotope signatures (respectively) for outlet and composite transects. Parameters removed from hypercube sampling included water content at -100 cm (W100 all layers); wilting point (all layers: WPz2, WPZ); field capacities and saturation capacities (all layers: SATz2, SATZ).

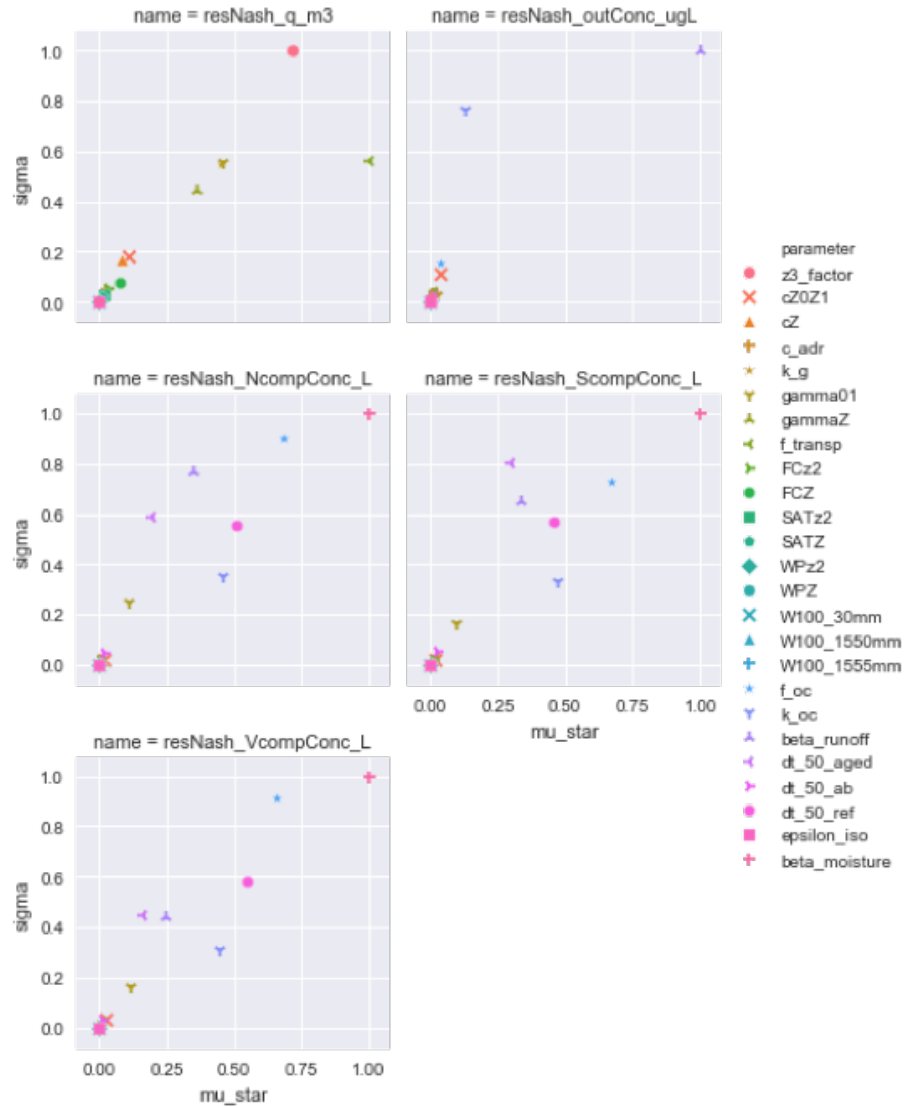


**Figure S5.** Morris sensitivity results for S-metolachlor concentrations at the outlet (top right) and composite soil transects (North, Valley and South). Discharge sensitivity ( $\text{m}^3$ ) is also shown (top left)

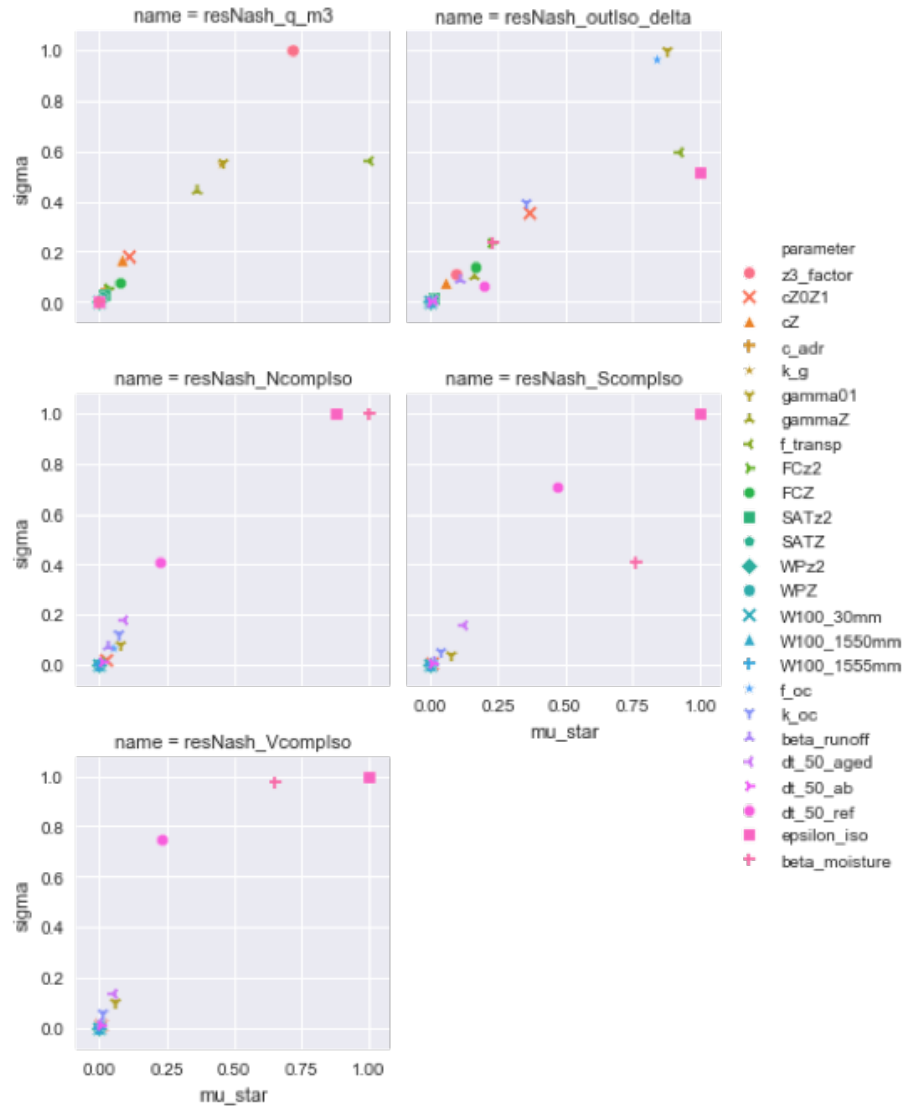


**Figure S6.** Morris sensitivity results for isotope signatures at the outlet (top right) and composite soil transects (North, Valley and South). Discharge sensitivity ( $\text{m}^3$ ) is also shown (top left)

# S11 Measured S-metolachlor concentrations and $\delta^{13}C$ for weekly transects

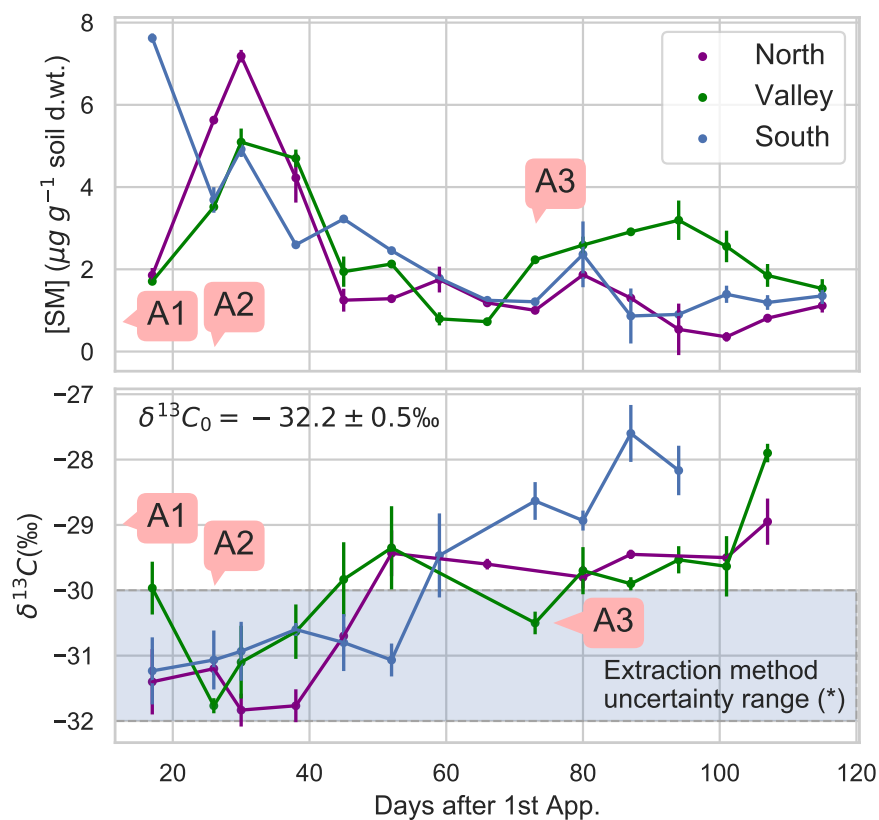


**Figure S7.** (Top) Measured S-metolachlor concentrations and (Bottom)  $\delta^{13}C$  for weekly transects. Confirmed applications A1, A2, and A3 (Table S2). (B) Shaded area indicates uncertainty range of the soil extraction method for S-metolachlor  $\delta^{13}C$  and within which no significant change from the application product's signature ( $\delta^{13}C_0$ ) may be concluded (Alvarez-Zaldivar et al., 2018).

## S12 $K_{OC}$ sensitivity

CSIA information in soils did not permit to reduce uncertainty for  $K_{OC}$  values across all sample resolutions. In a virtual experiment evaluating leaching extent based on  $DT_{50}$  and Koc correlation scenarios, Lindahl et al., (2008) find that when  $DT_{50}$  and  $K_{OC}$  were negatively correlated, larger variance in leaching extent was observed in the field, as lower degradation rates complement with higher mobility. In our study,  $DT_{50}$  and Koc values were negatively correlated ( $-0.47$ ,  $P < 0.001$ ), suggesting that spatial variations in organic carbon significantly altered mobility and degradation (Wu et al., 2012) as previously observed for S-metolachlor (Rice et al., 2002; Long et al., 2014). Namely, although catchment  $K_{OC}$  values below 500 L/Kg could be discarded on average (i.e., as shown by WIC models in bulk soils, Fig. S8), improvements in degradation parameter constraints based on temperature and moisture alone were not useful to constrain spatial variability of  $K_{OC}$  values (i.e., as shown by transect and plot  $K_{OC}$  distributions, Fig. S8). More detailed and explicit representation of organic carbon content evolution in both space and time using available information such as soil type, land-use and agricultural management (Meersmans et al., 2011), as it was done in this study for soil hydraulic properties, could further help constraining spatial variability of degradation rates and mobility parameters regulating pesticide leaching.

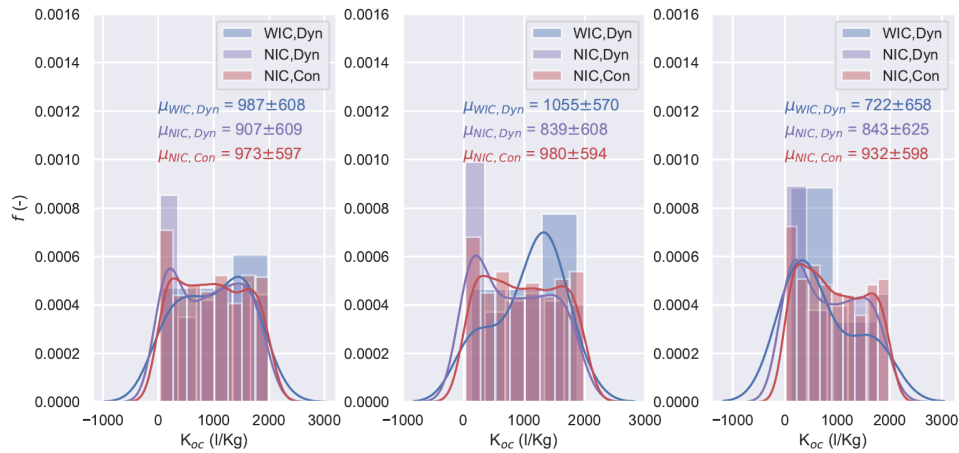


**Figure S8.** Distribution (out of a total of  $n = 2,500$  runs) of  $K_{OC}$  calibrated with no isotope constraint (NIC,  $n = 672$ ) and with isotope constraint (WIC,  $n = 244$ ) at three sampling resolutions (i.e., composite transect, transect and plot soils). NIC models considered  $KGE_{SM} > 0.5$  and  $KGE_Q > 0.5$ , while WIC models considered  $KGE_{SM} > 0.5$  and  $KGE_Q > 0.5$  and  $KGE_\delta > 0.8$ . Statistics for  $K_{OC}$  distributions are provided as mean (blue for WIC, purple and red for NIC, with  $DT_{50}$  dynamic depending of soil moisture and temperature or  $DT_{50}$  constant, respectively) and standard deviations ( $\mu \pm SD$ ).



- Ahuja, L. R. and Lehman, O. R.: The Extent and Nature of Rainfall-soil Interaction in the Release of Soluble Chemicals to Runoff, *J. Environ. Qual.*, 12, 34–40, <https://doi.org/10.2134/jeq1983.00472425001200010005x>, 1983.
- Alberts, E. E., Nearing, M. A., Wertz, M. A., Risse, L. M., Pierson, F. B., Zhang, X. C., Laflen, J. M., and Simanton, J. R.: Chapter 7. The soil component., in: USDA-Water Eros. Predict. Proj. Hillslope Profile Watershed Model Doc. NSERL Rep. 10, July 1995., 1995.
- 355 Allen, R. G., Pereira, L. S., Raes, D., and Smith, M.: Crop evapotranspiration: Guidelines for computing crop requirements, *Irrig. Drain. Pap. No. 56*, FAO, 300, <https://doi.org/10.1016/j.eja.2010.12.001>, 1998.
- Alvarez-Zaldívar, P., Payraudeau, S., Meite, F., Masbou, J., and Imfeld, G.: Pesticide degradation and export losses at the catchment scale: Insights from compound-specific isotope analysis (CSIA), *Water Res.*, 139, 198–207, <https://doi.org/10.1016/j.watres.2018.03.061>, 2018.
- National Center for Biotechnology Information (NCBI). PubChem Compound Database
- 360 Bakker, J. W., Boone, F. R., and Boekel, P.: Diffusie van gassen in grond en zuurstofdiffusiecoëfficiënten in Nederlandse akkerbouwgronden (Diffusion of gases in soil and oxygen diffusion coefficients in Dutch arable soils). Rapport 20, ICW, Wageningen, The Netherlands, 1987.
- Boesten, J. J. T. I.: Proposal for field-based definition of soil bound pesticide residues, *Sci. Total Environ.*, 544, 114–117, <https://doi.org/10.1016/j.scitotenv.2015.11.122>, 2016.
- 365 Boithias, L., Sauvage, S., Merlina, G., Jean, S., Probst, J. L., and Sánchez Pérez, J. M.: New insight into pesticide partition coefficient  $K_d$  for modelling pesticide fluvial transport: Application to an agricultural catchment in south-western France, *Chemosphere*, 99, 134–142, <https://doi.org/10.1016/j.chemosphere.2013.10.050>, 2014.
- Campolongo, F., Cariboni, J., and Saltelli, A.: An effective screening design for sensitivity analysis of large models, *Environ. Model. Softw.*, 22, 1509–1518, <https://doi.org/10.1016/j.envsoft.2006.10.004>, 2007.
- 370 Currie, J. A.: Gaseous diffusion in porous media. 2. Dry granular materials., *Br. J. Appl. Phys.*, 11, 318–324, 1960.
- Elsner, M.: Stable isotope fractionation to investigate natural transformation mechanisms of organic contaminants: principles, prospects and limitations., *J. Environ. Monit.*, 12, 2005–31, <https://doi.org/10.1039/c0em00277a>, 2010.
- European Commission: Review report for the active substance S-Metolachlor, EU Commission Health Consumer Protection Directorate General, 2004.
- 375 Fenech, C., Rock, L., Nolan, K., Tobin, J., and Morrissey, A.: The potential for a suite of isotope and chemical markers to differentiate sources of nitrate contamination: A review, *Water Res.*, 46, 2023–2041, <https://doi.org/10.1016/j.watres.2012.01.044>, 2012.
- Hunkeler, D., Meckenstock, R. U., Sherwood Lollar, B., Schmidt, T. C., Wilson, J. T., Schmidt, T., and Wilson, J.: A guide for assessing biodegradation and source identification of organic ground water contaminants using compound specific isotope analysis (CSIA), US EPA, Ada, 2008.
- 380 Hunt, R.: *Plant Growth Curves – The Functional Approach to Plant Growth.*, edited by: Arnold, E., Cambridge University Press (CUP), London, 248 pp., <https://doi.org/10.1017/s0014479700022857>, 1982.
- Jin, Y. and Jury, W. A.: Characterizing the Dependence of Gas Diffusion Coefficient on Soil Properties, *Soil Sci. Soc. Am. J.*, 60, 66–71, <https://doi.org/10.2136/sssaj1996.03615995006000010012x>, 1996.
- Kollman, W. and Segawa, R.: Interim Report of the Pesticide Chemistry Database, Environmental Protection Agency, US, California, 1995.
- 385 Lefrancq, M., Payraudeau, S., Guyot, B., Millet, M., and Imfeld, G.: Correction to Degradation and Transport of the Chiral Herbicide

- S-Metolachlor at the Catchment Scale: Combining Observation Scales and Analytical Approaches, *Environ. Sci. Technol.*, 52, 5517–5517, <https://doi.org/10.1021/acs.est.8b01118>, 2018.
- Leistra, M., van der Linden, A. M. A., Boesten, J. J. T. I., Tiktak, A., and van den Berg, F.: PEARL model for pesticide behaviour and emissions in soil-plant systems; Description of the processes in FOCUS PEARL v 1.1.1., Bilthoven, Natl. Inst. Public Heal. Environ. Wageningen, Alterra, Green World Res. RIVM Rep. 711401009/Alterra-rapport 013; 116 blz.; 9 fig.; 1 tab.; 42 ref., 2001.
- Lim, K. J., Engel, B. A., Muthukrishnan, S., and Harbor, J.: Effects of initial abstraction and urbanization on estimated runoff using CN technology, *J. Am. Water Resour. Assoc.*, 42, 629–643, <https://doi.org/10.1111/j.1752-1688.2006.tb04481.x>, 2006.
- Lindahl, A. M. L., Söderström, M. and Jarvis, N.: Influence of input uncertainty on prediction of within-field pesticide leaching risks. *J. Contam. Hydrol.* 98, 106, <https://doi.org/10.1016/j.jconhyd.2008.03.006>, 2008.
- Long, Y. H., Li, R. Y. and Wu, X. M.: Degradation of S-metolachlor in soil as affected by environmental factors. *J. Soil Sci. Plant Nutr.*, 14, 189-198, <http://dx.doi.org/10.4067/S0718-95162014005000015>, 2014.
- Manfreda, S., Fiorentino, M., and Iacobellis, V.: DREAM: a distributed model for runoff, evapotranspiration, and antecedent soil moisture simulation, *Adv. Geosci.*, 2, 31–39, <https://doi.org/10.5194/adgeo-2-31-2005>, 2005.
- McGrath, G. S., Hinz, C., and Sivapalan, M.: Modeling the effect of rainfall intermittency on the variability of solute persistence at the soil surface, *Water Resour. Res.*, 44, 1–10, <https://doi.org/10.1029/2007WR006652>, 2008.
- Meersmans, J., Van Wesemael, B., Goidts, E., Van Molle, M., De Baets, S., De Ridder, F.: Spatial analysis of soil organic carbon evolution in Belgian croplands and grasslands, 1960-2006. *Glob. Change Biol.*, 17, 466-479. <https://doi.org/10.1111/j.1365-2486.2010.02183.x>, 2011.
- Millington, R. J. and Quirk, J. P.: Transport in porous media, *Trans. 7th Int. Congr. Soil Sci.*, 1, 97–106, 1960.
- Morris, M. D.: Factorial sampling plans for preliminary computational experiments, *Technometrics*, 33, 161–174, <https://doi.org/10.2307/1269043>, 1991.
- Neitsch, S. L., Arnold, J. G., Kiniry, J. R., and Williams, J. R.: Soil and Water Assessment Tool. Theoretical Documentation. Version 2009. Texas Water Resources Institute Technical Report No. 406 Texas A and M University System College Station, Texas, USA. 647 pages, 2011.
- Nestler, A., Berglund, M., Accoe, F., Duta, S., Xue, D., Boeckx, P., and Taylor, P.: Isotopes for improved management of nitrate pollution in aqueous resources: Review of surface water field studies, *Environ. Sci. Pollut. Res.*, 18, 519–533, <https://doi.org/10.1007/s11356-010-0422-z>, 2011.
- Prasad, R.: A linear root water uptake model, *J. Hydrol.*, 99, 297–306, [https://doi.org/10.1016/0022-1694\(88\)90055-8](https://doi.org/10.1016/0022-1694(88)90055-8), 1988.
- Raes, D.: BUDGET: a Soil Water and Salt Balance Model. Reference manual. Version 5.0., Catholic University of Leuven, Leuven, Belgium, 2002.
- Rayleigh, L. S.: Theoretical considerations respecting the separation of gases by diffusion and similar processes, *Philos. Mag.*, 42, 493–498, <https://doi.org/10.1080/14786449608620944>, 1896.
- Rémy, J. C. and Marin-Lafèche, A.: L'analyse de terre : réalisation d'un programme d'interprétation automatique., *Ann. Agron.*, 25, 607–632, 1974.
- Rice, P. J., Anderson, T. A. and Coats, J. R.: Degradation and persistence of metolachlor in soil: effects of concentration, soil moisture, soil depth, and sterilization. *Environ. Toxicol. Chem. / SETAC* 21, 2640-8. <https://doi.org/10.1002/etc.5620211216>, 2002.
- Saxton, K. E. and Rawls, W. J.: Soil Water Characteristic Estimates by Texture and Organic Matter for Hydrologic Solutions, *Soil Sci. Soc. Am. J.*, 70, 1569–1578, <https://doi.org/10.2136/sssaj2005.0117>, 2006.

- 425 Schroll, R., Becher, H. H., Dörfler, U., Gayler, S., Grundmann, S., Hartmann, H. P., and Ruoss, J.: Quantifying the effect of soil moisture on the aerobic microbial mineralization of selected pesticides in different soils, *Environ. Sci. Technol.*, 40, 3305–3312, <https://doi.org/10.1021/es052205j>, 2006.
- Sheikh, V., Visser, S., and Stroosnijder, L.: A simple model to predict soil moisture: Bridging Event and Continuous Hydrological (BEACH) modelling, *Environ. Model. Softw.*, 24, 542–556, <https://doi.org/10.1016/j.envsoft.2008.10.005>, 2009.
- 430 Sherwood Lollar, B., Slater, G. F., Sleep, B., Witt, M., Klecka, G. M., Harkness, M., and Spivack, J.: Stable carbon isotope evidence for intrinsic bioremediation of tetrachloroethene and trichloroethene at Area 6, Dover Air Force Base, *Environ. Sci. Technol.*, 35, 261–269, <https://doi.org/10.1021/es001227x>, 2001.
- Shi, X. N., Wu, L. S., Chen, W. P., and Wang, Q. J.: Solute Transfer from the Soil Surface to Overland Flow: A Review, *Soil Sci. Soc. Am. J.*, 75, 1214–1225, <https://doi.org/DOI.10.2136/sssaj2010.0433>, 2011. Soil Conservation Service: Soil Conservation Service. Section
- 435 4 Hydrology, in: *Natl. Eng. Handbook*, SCS. Soil, 1972.
- USDA.: Revised Universal Soil Loss Equation. Version 2. (RUSLE2)., Springer-Verlag, 2003.
- Walker, A.: A Simulation Model for Prediction of Herbicide Persistence, *J. Environ. Qual.*, 3, 396–401, <https://doi.org/10.2134/jeq1974.00472425000300040021x>, 1974.
- Wu, X., Li, M., Long, Y. and Liu, R.: Effects of adsorption on degradation and bioavailability of metolachlor in soil. *J. Soil Sci. Plant*
- 440 *Nutr.*, 11, 83-97. <http://dx.doi.org/10.4067/S0718-95162011000300007>, 2011.